

Experimental and Modeling Studies of Halogen Fire Suppression Chemistry

Andrew McIlroy
Mechanics and Materials Technology Center
The Aerospace Corporation
Los Angeles, California 90009-2957

Introduction

Halons achieve superior fire suppression performance due to chemical as well as physical fire suppression mechanisms. Many of the proposed halon replacements display relatively little chemical fire suppression compared to Halon 1301 (CF_3Br). One promising alternative for many applications are iodine containing compounds, of which CF_3I is a prime example. Past experimental investigations of iodine based fire suppression have shown performance for iodine containing compounds that is similar to that of the analogous bromine compounds, but slightly poorer. However, chemical models have given the opposite result, that iodine compounds are superior to bromine compounds? Here we investigate this question using a modified form of Westbrook's CF_3X model.

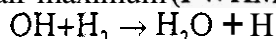
Model Description

The Sandia PREMIX laminar flame code^{3,4} has been used to calculate the flame structure for freely propagating, atmospheric pressure, hydrogen-oxygen flames doped with CF_3X ($\text{X}=\text{Br},\text{I}$). The results presented here are for a 9:19:72 $\text{H}_2:\text{O}_2:\text{Ar}$ mixture doped with varying concentrations of CF_3X . This gas $\text{H}_2/\text{O}_2/\text{Ar}$ flame is chosen to match experimental conditions investigated in our laboratory; safety considerations preclude the use of higher H_2 concentrations. The pressure is 1.00 atm, and the initial temperature is 298 K. The reaction mechanism and rate constants are presented in Table I. All calculations were carried out over an interval of -1.00 to 2.00 cm; the plots of results are shown over the most interesting regions and do not reflect the limits of the calculation. The chemical kinetic reaction rate model has been described previously. Briefly, it is based on the hydrogen oxidation reaction mechanism of Thorne *et al.*⁶ and the CF_3Br combustion reaction mechanism of Westbrook. Iodine compound reaction rates are substituted for the bromine compound reaction rates to compose the CF_3I reaction mechanism.

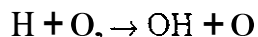
Results

Undoped H₂O, Flame

For comparison, the results of a calculation with no CF_3X are shown in Figure 1. The maximum flame temperature achieved is 1229 K (close to the 1234 K adiabatic flame temperature), and the burning rate is 5.40 cm s^{-1} . The flame width is approximately 0.07 cm, measured from the full-width-at-half-maximum (FWHM) of the reaction



rate of progress. As expected, this reaction dominates the flame along with the chain branching reaction



Water is the only major product, and the fraction of unburned hydrogen fuel is $1.34 \times 10^{-4}\%$ in the post flame gases.

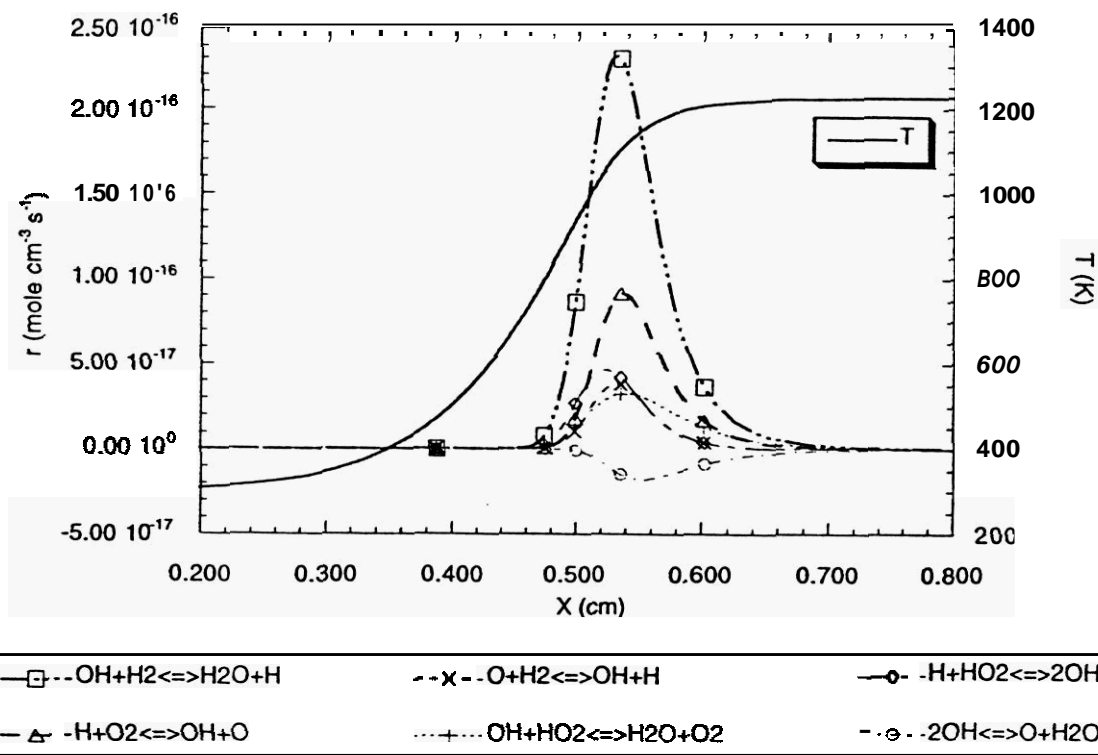


Figure 1: Unperturbed flame rates of progress.

CF₃Br Doped Flame

For ~~the~~ 0.1% CF₃Br doped flame, the maximum flame temperature is **1254 K**, and the flame zone is 0.08 cm wide measured ~~as~~ for the undoped case. The burning rate is 1.77 cm s⁻¹. In the post flame zone, 2.9×10⁻⁵% of the H₂ remains unburned. Figures 2 and 3 display the calculated halogen containing species mole fractions ~~as~~ as a function of a function of spatial position.

The chemistry of CF₃Br in the flame is dominated by thermal decomposition (see Figure 4). The weak Br-C bond ruptures ~~to~~ to give Br-atoms and CF₃-radicals. All other CF₃Br chemical reactions ~~are~~ are slow compared to thermal decomposition. Abstraction of bromine by hydrogen atoms does ~~take~~ take place, but is approximately six orders of magnitude slower than thermal decomposition throughout most of the flame. Only ~~at~~ at temperatures below 1000 K is hydrogen abstraction favored over thermal decomposition, and below 1000 K, both ~~are~~ are slow processes. The initial thermal decomposition provides ~~a~~ a heat sink in the flame and also opens new chemical pathways involving the bromine atom and CF₃ radical.

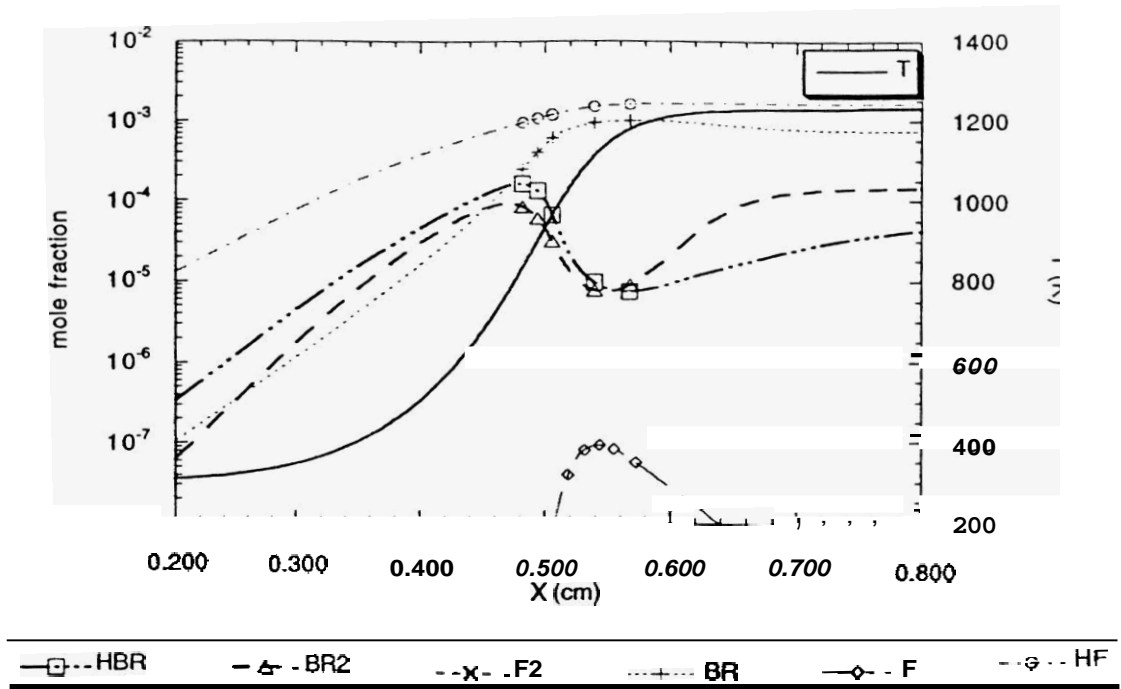


Figure 2: HX (X=F, Br) mole fractions.

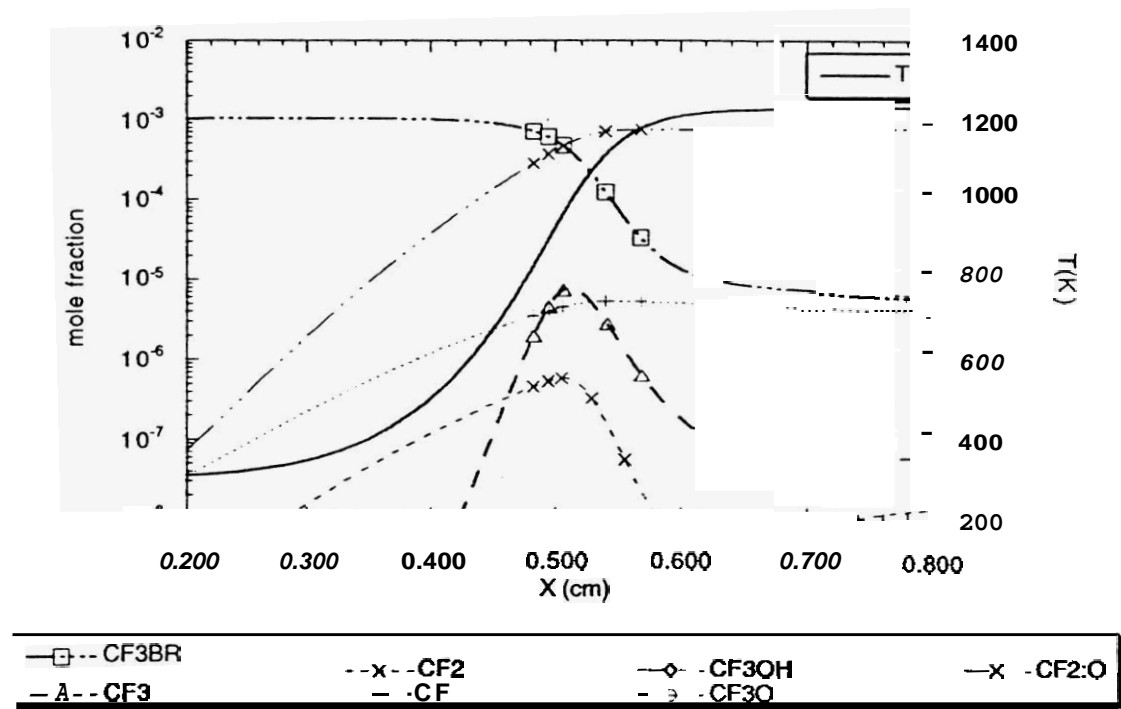


Figure 3: Mole fractions of $CF_nBr_mO_l$ species.

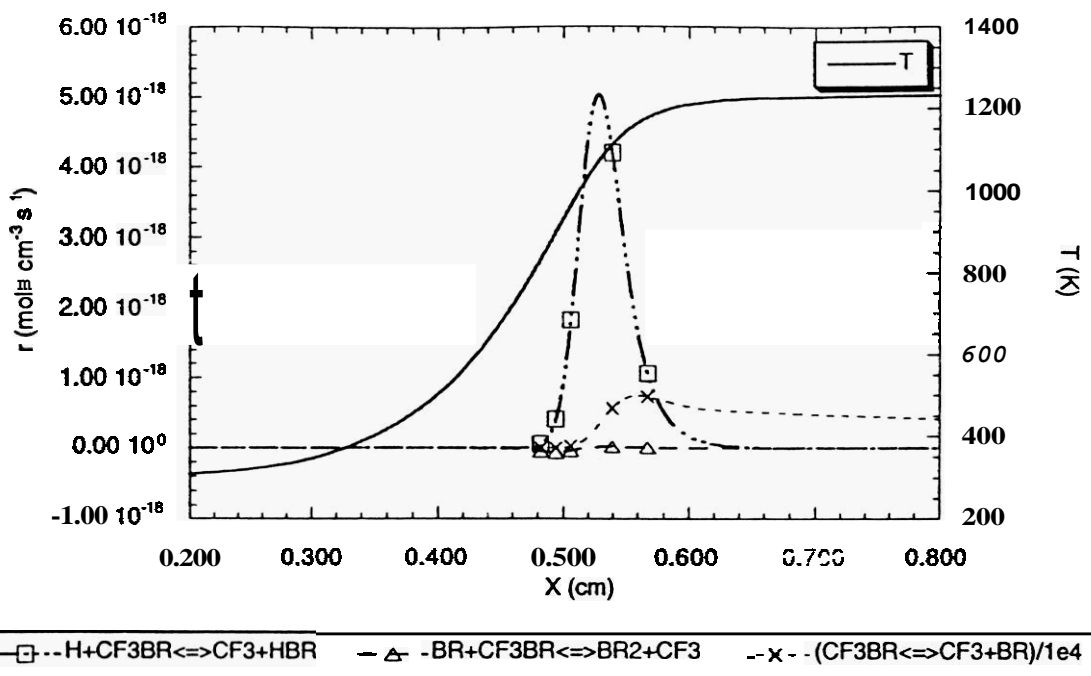
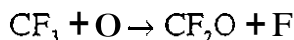


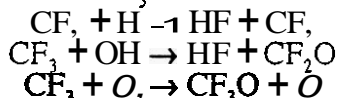
Figure 4 CF_3Br reaction rates of progress. Note that CF_3Br unimolecular dissociation rate is divided by 10^4 .

The bromine atoms released into the flame undergo a variety of reactions (see Figure 6). Their ultimate fate in the post flame gases is as Br-atoms (65%), Br_2 (23%) and HBr (12%). The HBr is formed by the reaction of Br-atoms with HO, and H_2 .

The CF₃ radicals by thermal decomposition of CF_3Br are consumed in reactions with H-atoms, O-atoms, O_2 , and OH-radicals (see Figure 5). Of these reactions, the O-atom channel,

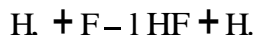


is dominant and occurs only in the hottest portion of the flame. Perfluoroformaldehyde is stable and reacts slowly with H-atoms and OH-radicals. The yield of CF_2O from CF_3Br during combustion is 81%. The perfluoroformaldehyde accounts for 54% of the total fluorine in the post-flame gas. Other active CF_3 reaction channels are



Thermal decomposition of CF_3O yields CF_2O (see Figure 7). The CF₃ and CF_3O radicals are removed by reaction with H, O, and OH radicals giving products of HF, CFO, and CF (see Figure 8). Further reaction with H, O, and OH yields HF, CO, and CO_2 .

Of the F-atoms produced in the decomposition of CF_3Br , >99% are consumed by reaction with H_2



Hydrofluoric acid accounts for 46% of the total fluorine. Of the total HF produced, 38% results from the destruction of CF_2O and the remainder arises from F-atom hydrogen abstraction. Thus the products HF and CF_2O represent >99.9% of the fluorine introduced into the flame by CF_3Br .

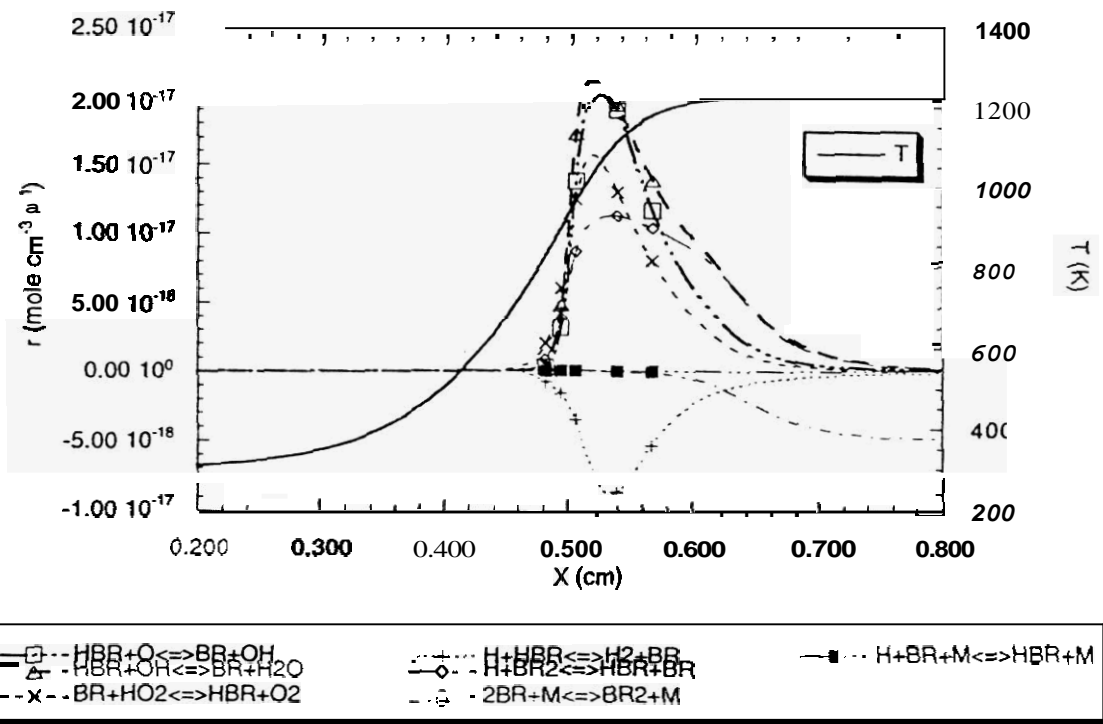


Figure 6: HBr, Br, Br₂ reaction rates of progress.

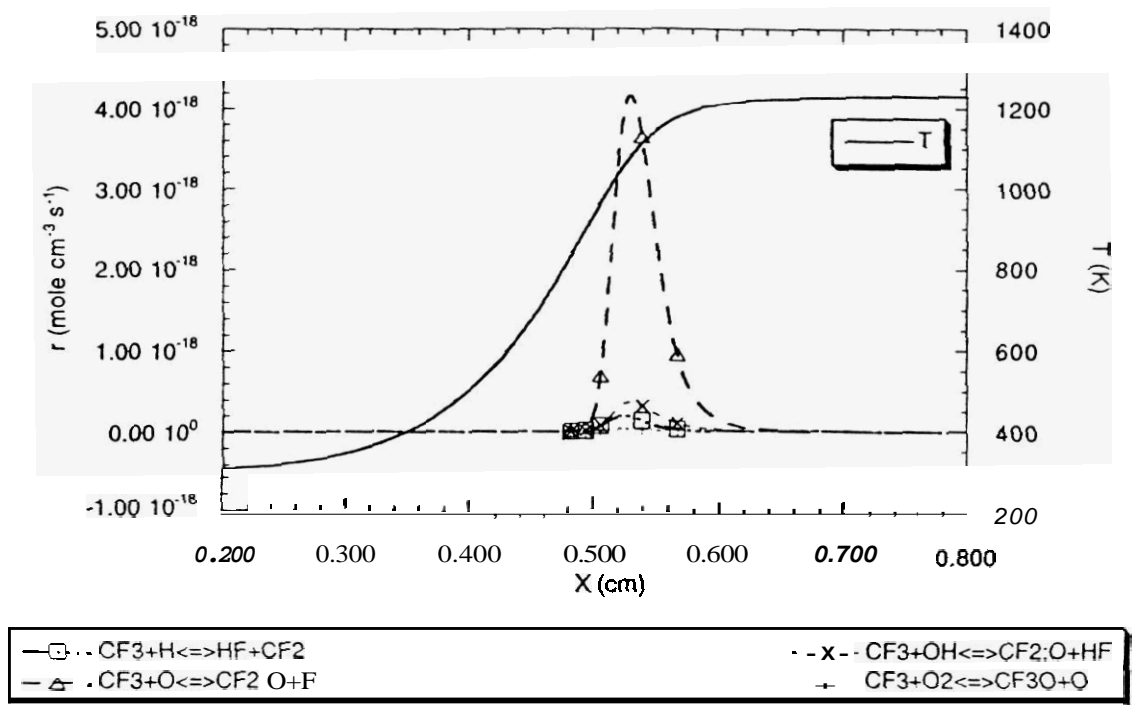


Figure 5: CF, reaction rates of progress.

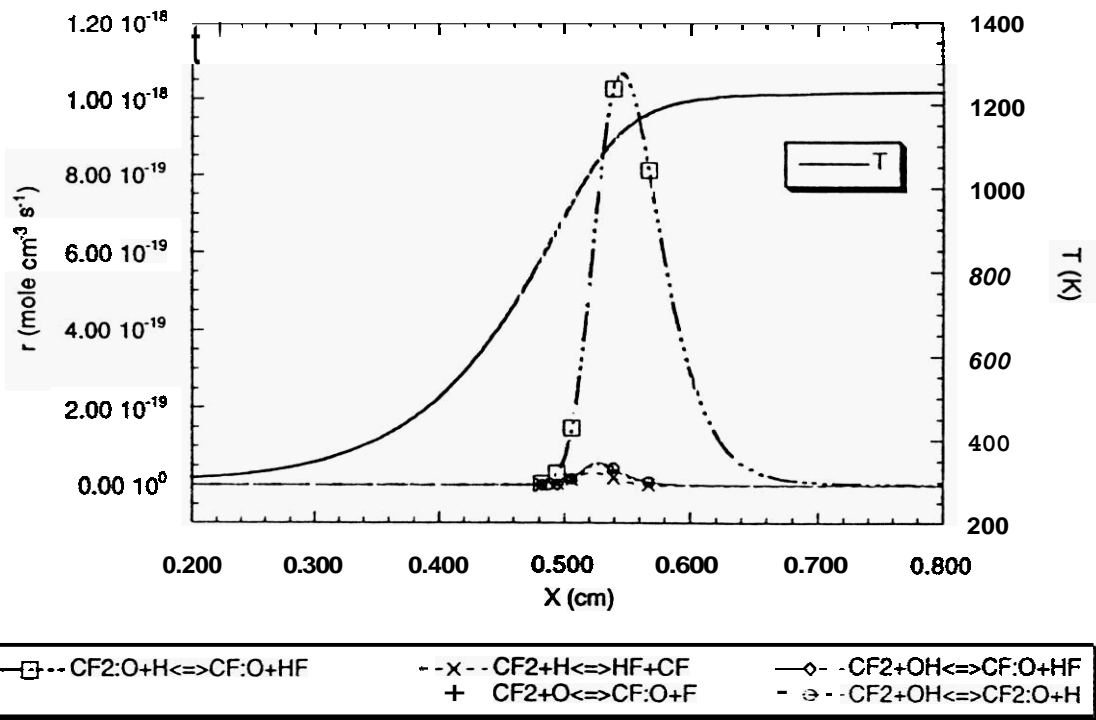


Figure 7: CF, and CF₂O reaction rates of progress.

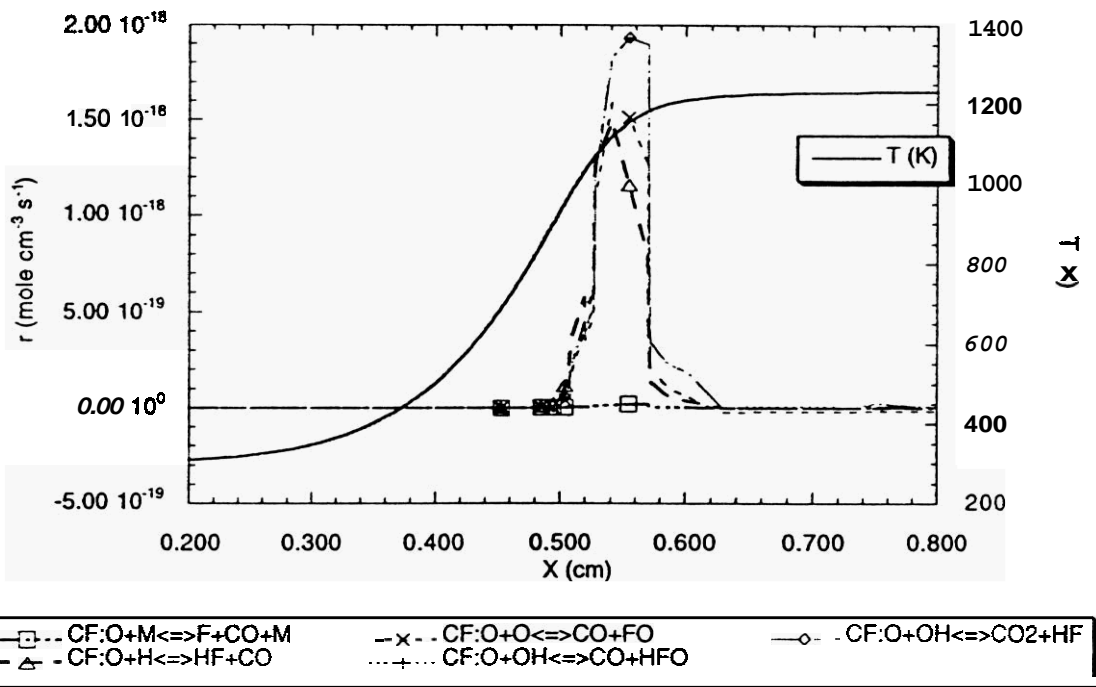
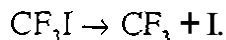


Figure 8: CFO reaction rates of progress.

CF₃I Doped Flame

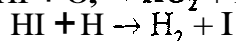
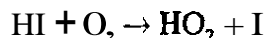
For the 0.1% CF₃I doped flame, the maximum flame temperature is **1239 K**, and the flame zone is **0.06 cm** wide measured **as** for the undoped case. The burning rate is **4.32 cm s⁻¹**. In the post flame zone, 0.095% of the H₂ remains unburned. Figures **9** and **10** show the halogen containing species mole fractions **as** a function of flame height for this flame.

Rate of progress plots show that CF₃I, like CF₃Br, is primarily destroyed in the flame by unimolecular dissociation



This process **takes** place very early in the flame where the temperature exceeds **-750 K**. Hydrogen atom abstraction of iodine contributes very little to CF₃I destruction since the CF₃I is **thermally** decomposed before high enough temperatures **are** reached to support the required H-atom concentrations.

Following dissociation, the iodine atoms participate in several reactions (see Figure 10). However, the plots of species concentration show that the I-atoms **are** the primary iodine-containing species in the flame after CF₃I decomposition, accounting for **>99.9%** of the iodine. Very early in the flame (**0.354-0.356 cm**), the HI concentration **peaks**; this species is consumed **at** low temperatures by reaction with O₂ and **at** higher temperatures by reaction with H-atoms.



Hydroxyl radicals also plays a small role in HI consumption.

The combustion process and **fate** of the CF₃ fragment in the CF₃I doped flame is very similar to that described for the CF₃Br doped flame. However, the quantitative yield of products is different. In the CF₃I doped flame, CF₂O accounts for **76%** of the carbon from CF₃I and **50.4%** of **the** fluorine. The remaining **49.6%** of of the fluorine is converted to HF.

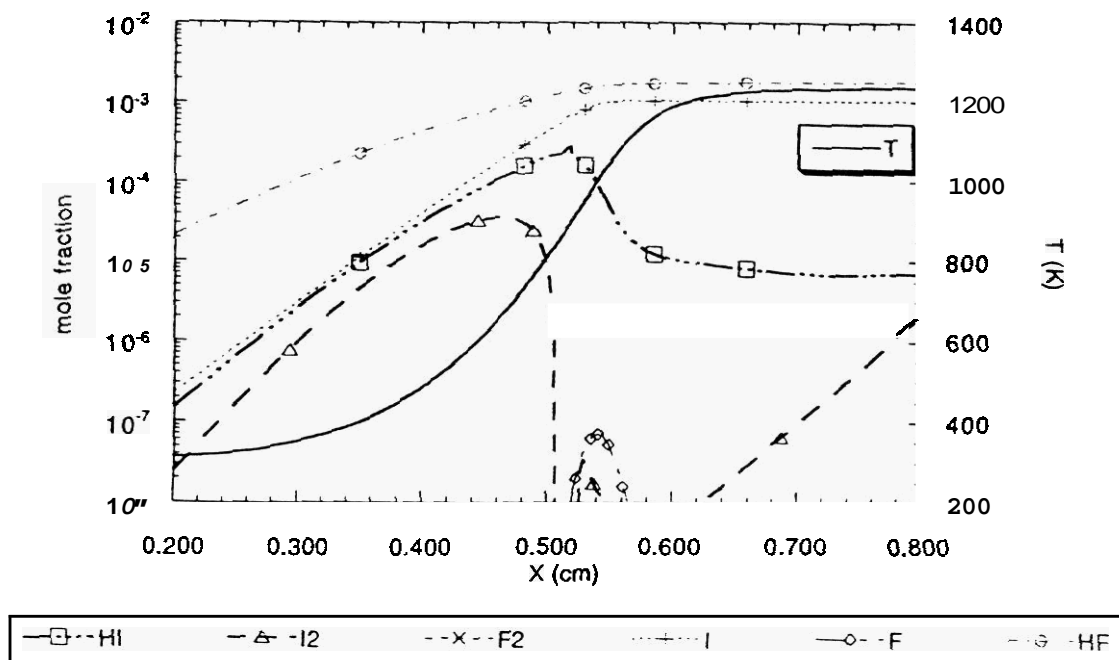


Figure 9: HX (X=F, I) mole fractions.

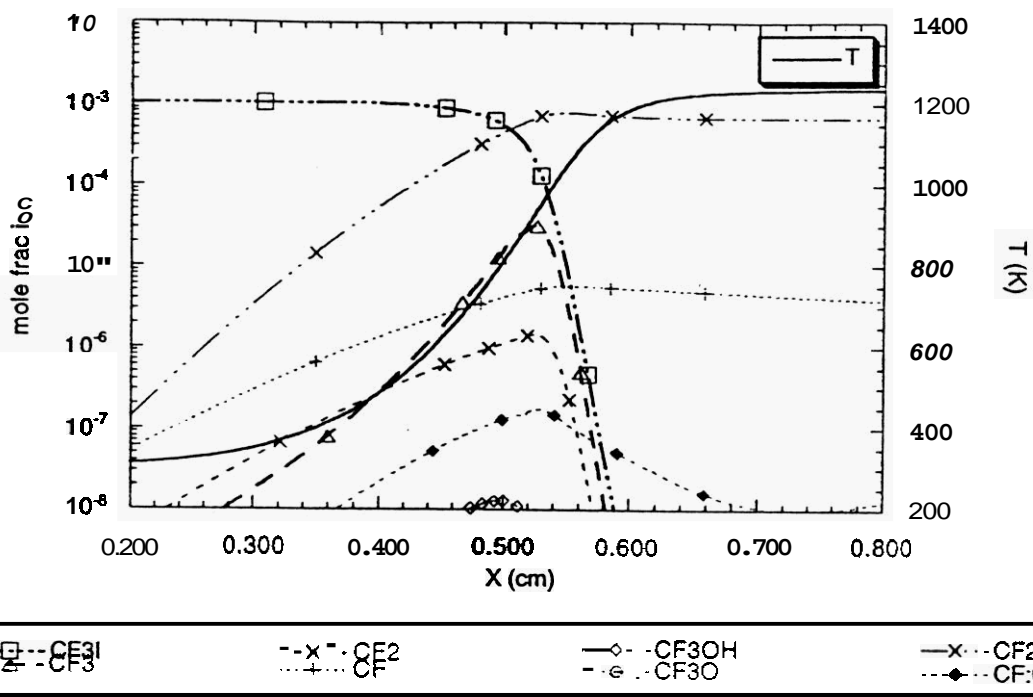


Figure 11: $CF_n I_m O_l$ mole fractions.

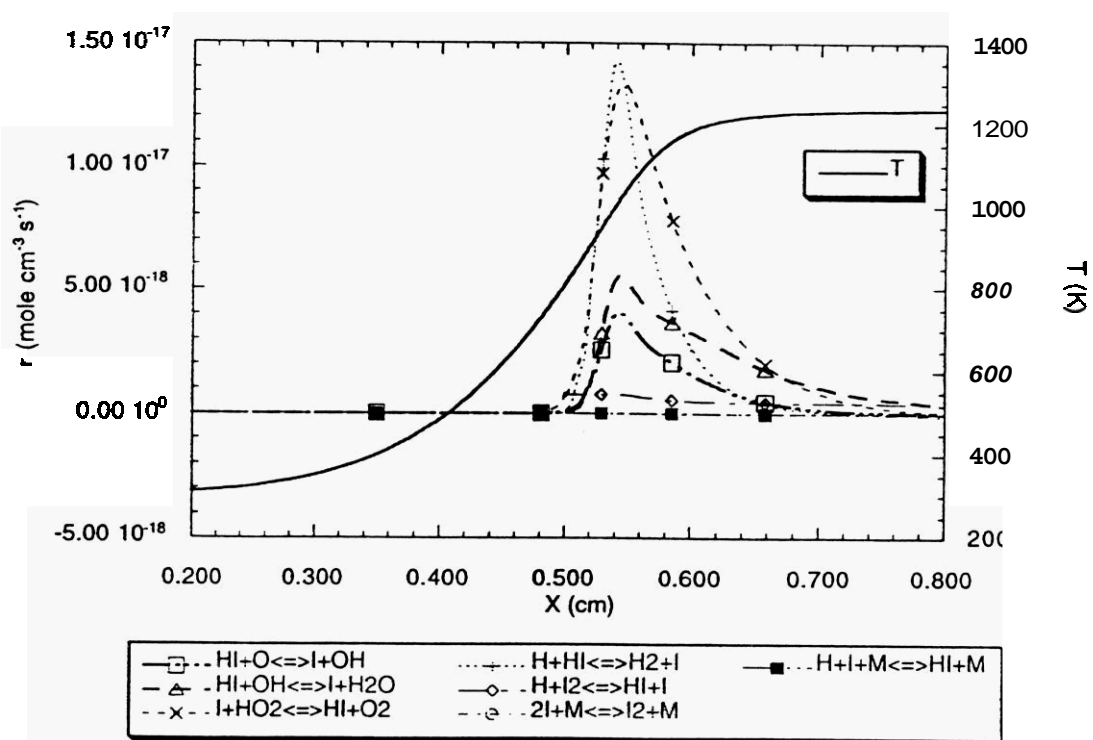


Figure 10: HI, I, and I_2 reaction rates of progress

Discussion

Comparison of Doped Flame Calculations

Table I lists the flame temperatures, burning velocities, and flame widths of the three H_2/O_2 flames doped with 0.1% CF_3X ($\text{X}=\text{I}, \text{Br}$) presented above. Figure 12 displays the variation of burning velocity and flame temperature as a function of CF_3X concentration in the hydrogen flame discussed here. At a concentration of 0.1% CF_3Br , the flame is strongly inhibited with a 50% reduction in flame speed and wider flame zone than the undoped flame. By contrast CF_3I requires approximately three times the concentration to reach a similar level of inhibition.

	T_{flame} (K)	v_{flame} (cm s^{-1})	width (cm)
Undoped Flame	1229	5.40	0.07
4% CF_3Br	1235	2.604	0.08
4% CF_3I	1239	4.32	0.06

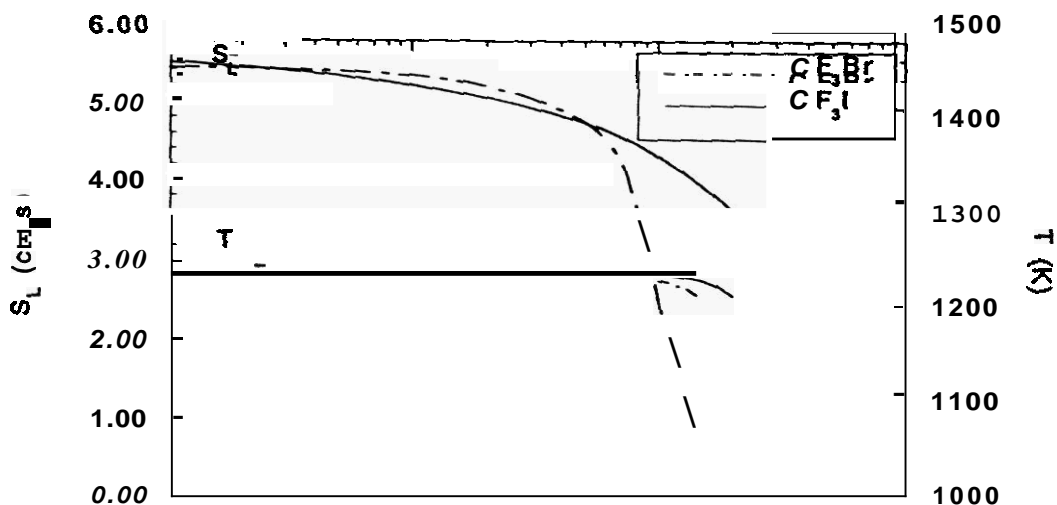
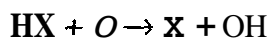
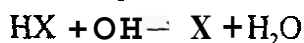
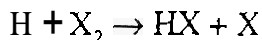
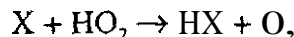


Figure 12: Burning velocity and flame temperature as a function of CF_3X ($\text{X}=\text{Br}, \text{I}$) doped $\text{H}_2/\text{O}_2/\text{Ar}$ flame.

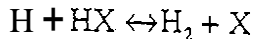
Comparison of the iodine and bromine chemistry in the 10% hydrogen flame shows several key differences; Figure 13 displays a schematic rendering of the differences between the iodine and bromine reaction pathways. The reactions



are slower for iodine compared to bromine by 0.1, 0.7, and 0.5 respectively. However, the reaction



is twice as fast for iodine compared to bromine. The hydrogen abstraction reaction



proceeds in the forward direction for iodine, but the reverse for bromine. Finally, unimolecular dissociation of the X, is unimportant for iodine, but is observed for bromine.

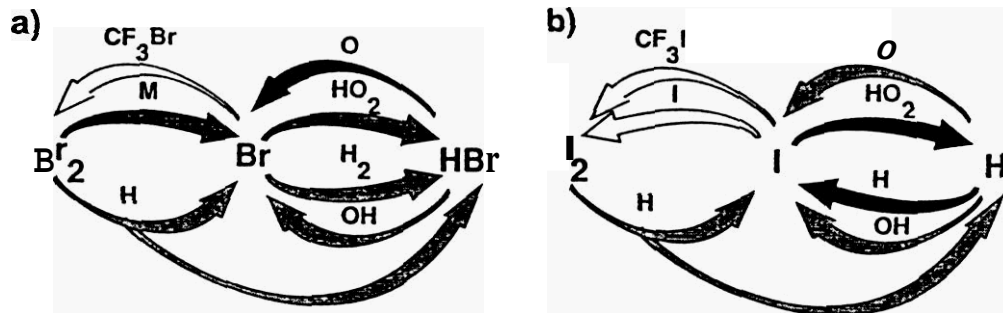
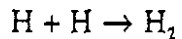
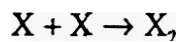
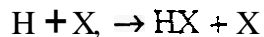
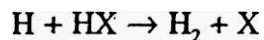


Figure 13: Bromine and iodine reaction mechanism. Arrows show direction of reaction and shading indicates relative rate, darker is faster.

The lack of X, unimolecular dissociation for iodine in the rate of progress plots is largely due to the lack of I_2 . At flame temperatures, molecular iodine is essentially completely dissociated. Without iodine recombination, the catalytic hydrogen recombination cycle proposed by Westbrook² cannot operate for iodine.



Breaking this cycle may account for the lower fire suppression performance observed for CF_3I compared to CF_3Br in past experiments' **and** in the present calculations.

Since the C-Br and C-I bond is very weak, **and** Br-F **and** I-F bonds **are** not formed, the reaction of the CF_3 radicals produced in the unimolecular decomposition of the CF_3X is largely decoupled from the iodine or bromine chemistry. Figure 14 outlines the CF_3 destruction mechanism. In this **figure**, the darker arrows indicate faster reactions, measured **at** the peak values in the rate of progress plots. The destruction of CF_3 , proceeds primarily through CF_2O **and** leads ultimately to the formation of CO or CO, **as well as** HF. The CF_3 -radicals have little catalytic inhibition effect on **the** hydrogen-oxygen flame. Although they act to consume O-atoms, subsequent reaction of the F-atoms produced with H, leads to the formation of reactive H-atoms. However, they **are** a hydrogen sink, converting H-atoms to HF.

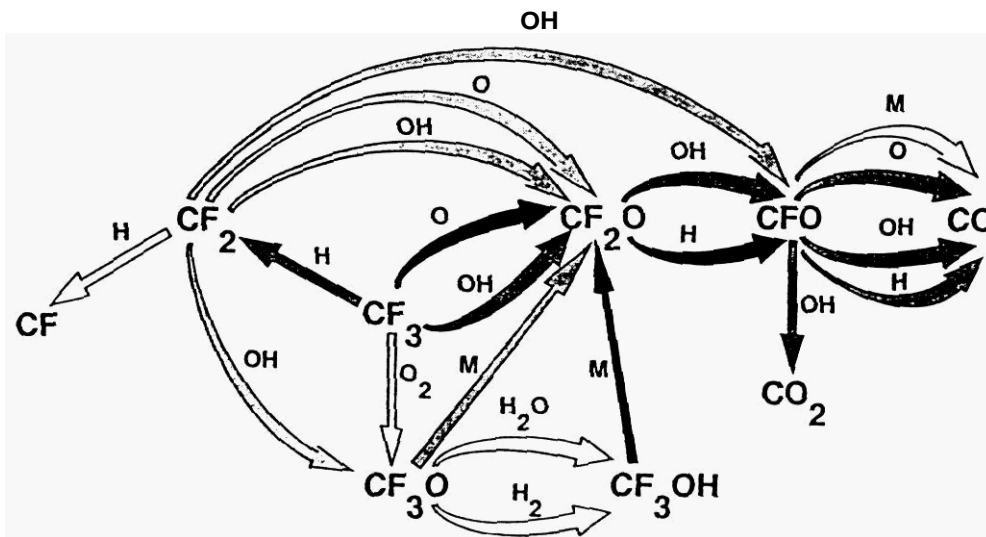


Figure 14: CF, destruction mechanism. Arrows show direction of reaction and shading indicates relative maximum rates where black is fastest.

One of the practical concerns for a fire suppressant, beyond fire suppression performance, is the nature of the combustion byproducts that are formed when it is applied to a flame. Perfluorocarbons and hydrofluorocarbons have recently been shown to produce large and potentially harmful concentrations of HF during flame extinguishment. The agent CF_3I will have byproducts similar to CF_3Br . The fluorine will be converted to HF and COF, in the flame. Perfluoroformaldehyde is readily converted to HF in water and has toxic and corrosive hazard ratings similar to HF. The iodine in CF_3I exists as I-atoms in the flame, as it cools it will recombine to form a variety of iodine compounds depending on the reaction products available in the post flame gases. Certainly, I_2 and HI will result from the simple hydrogen flame presented here. In a more complex hydrocarbon flame in which not all of the fuel is fully oxidized, organic iodine compounds would also be expected.

Acknowledgements

Support for this work was provided by the Aerospace Sponsored Research program and the Air Force Space and Missile Systems Center Office of Environmental Management. The author would like to thank Dr. Brian Brady and Dr. Bob Martin of the Aerospace Corporation, Dr. James Flemming of the Naval Research Laboratory, and Prof. Paul Ronney of the University of Southern California for many helpful discussions

References

¹ Sheinson, R. S., Penner-Hahn, J. E., and Indritz, D., *Fire Safety Journal* 15,437 (1989).

² Westbrook, C. K., *Nineteenth Symposium (International) on Combustion*, The Combustion Institute, Pittsburgh, PA, 127 (1982).

³ Kee, R. J., Grcar, J. F., Smooke, M. D., and Miller, J. A., *A Fortran Program for Modeling Steady Laminar One-Dimensional Premixed Flames*, Sandia National Laboratories Report No. SAND85-8240.UC-4, 1987.

⁴ Kee, R. J., Rupley, F. M., and Miller, J. A., *Chemkin II: A Fortran Chemical Kinetics Package for the Analysis of Gas-Phase Chemical Kinetics*, Sandia National Laboratories Report No. SAND89-8009.UC-401, 1991.

⁵ McIlroy, A. and Johnson, L. K., *Combustion Science and Technology* in press (1996).

⁶ Thorne, L. R., Branch, M. C., Chandler, D. W., Kee, R. J., and Miller, J. A., *Twenty-First Symposium (International) on Combustion*, The Combustion Institute, Pittsburgh, 1986, pp. 965-911.

Westbrook, C. K., *Combustion Science and Technology* 34201-225 (1983).